Zero-temperature ordering dynamics in a two-dimensional biaxial next-nearest-neighbor Ising model

Soham Biswas and Mauricio Martin Saavedra Contreras
Departamento de Física, Universidad de Guadalajara, Guadalajara, Jalisco, Mexico

(Received 11 June 2019; published 22 October 2019)

We investigate the dynamics of a two-dimensional biaxial next-nearest-neighbor Ising model following a quench to zero temperature. The Hamiltonian is given by $H = -J_0 \sum_{i,j=1}^{L}[(S_{i,j}S_{i+1,j} + S_{i,j}S_{i,j+1}) - \kappa(S_{i,j}S_{i+2,j} + S_{i,j}S_{i,j+2})]$. For $\kappa < 1$, the system does not reach the equilibrium ground state and keeps evolving in active states forever. For $\kappa \geqslant 1$, though, the system reaches a final state, but it does not reach the ground state always and freezes to a striped state with a finite probability like a two-dimensional ferromagnetic Ising model and an axial next-nearest-neighbor Ising (ANNNI) model. The overall dynamical behavior for $\kappa > 1$ and $\kappa = 1$ is quite different. The residual energy decays in a power law for both $\kappa > 1$ and $\kappa = 1$ from which the dynamical exponent z has been estimated. The persistence probability shows algebraic decay for $\kappa > 1$ with an exponent $\theta = 0.22 \pm 0.002$ while the dynamical exponent for ordering $z = 2.33 \pm 0.01$. For $\kappa = 1$, the system belongs to a completely different dynamical class with $\theta = 0.332 \pm 0.002$ and $z = 2.47 \pm 0.04$. We have computed the freezing probability for different values of κ. We have also studied the decay of autocorrelation function with time for a different regime of κ values. The results have been compared with those of the two-dimensional ANNNI model.

DOI: 10.1103/PhysRevE.100.042129

I. INTRODUCTION

When a system is close to the critical point, anomalies can occur in a large variety of dynamical properties, and models having identical static critical behavior may display different behavior when dynamic critical phenomena are considered [1]. Some of the dynamical phenomena which have attracted a lot of attention are critical dynamics, quenching and coarsening, reaction diffusion systems, random walks, etc. Recently, considerable interest has been developed for studying the dynamics of Ising spin systems which has emerged as a rich field of present-day research [2,3]. The fate and the behavior of Ising spin systems following a deep quench below the critical temperature have been one of the central topics of interest in the study of the nonequilibrium dynamics for the last two decades. In a quenching process, the system has a disordered initial configuration which corresponds to a very high temperature ($T \to \infty$) and its temperature is suddenly dropped. Systems quenched from a disordered phase into an ordered phase do not order instantaneously. Instead, the length scale of ordered regions grows with time as the different broken symmetry phases compete with each other to select the equilibrium state [4].

In a quenching process, the initial configuration of the system is a configuration of uncorrelated spins, which evolve by zero-temperature Glauber dynamics [5], corresponding to a quench from $T \to \infty$ to $T = 0$. This involves picking up a spin at random and computing the change of energy ΔE which is essentially $E_{\text{flipped}} - E_{\text{present}}$. If $\Delta E < 0$ (>0), the spin will (will not) flip and for $\Delta E = 0$, the spin flip will happen with probability $1/2$. After each update, time is updated by $1/L^d$, such that on average, each spin undergoes one update attempt in a single time unit.

A zero-temperature quench of one-dimensional Ising model with nearest-neighbor interaction ultimately leads to the equilibrium configuration, i.e., all spins point up (or down). The system evolves according to the Glauber dynamics resulting in quite a few interesting phenomena like domain growth [4,6], persistence [7–11], etc. The average domain size D increases in time t as $D(t) \sim t^{1/z}$, where z is the dynamical exponent associated with the growth. Apart from the domain growth phenomenon, another important dynamical behavior which has been commonly studied is persistence, the tendency of a spin to remain in its original state following a quench to zero temperature [7,8]. In a zero-temperature quench of Ising model, persistence shows a power law behavior, i.e., $P(t) \sim t^{-\theta}$. θ is called the persistence exponent and is unrelated to any other known static or dynamic exponents [7,9]. In two or higher dimensions, however, following a quench to zero temperature the system does not always reach the ground state [11], although these scaling relations still hold good.

Dynamical behavior of Ising spin systems changes drastically in the presence of competing interactions. To study the effect of the competing interaction on the dynamical behavior, the simple Ising model with a competing next-nearest-neighbor interaction has been studied earlier in both one and two dimensions [12–15]. Competing interactions could also be present in the system if spins have random long range interactions which are quenched in nature [16,17].

In one dimension, the simplest example of Ising spin system with competing interaction is the ANNNI (axial next-nearest-neighbor Ising) model with L spins which can be

described by the Hamiltonian

$$H = -J \sum_{i=1}^{L} (S_i S_{i+1} - \kappa S_i S_{i+2}).$$

In this model it was found that for $\kappa < 1$, under a zero-temperature quench with single spin flip Glauber dynamics, the system does not reach its true ground state. (The ground state is ferromagnetic for $\kappa < 0.5$, antiphase for $\kappa > 0.5$, and highly degenerate at $\kappa = 0.5$ [18].) On the other hand, after some initial short time, the number of domain walls does not decay but remain mobile at all times. That makes the persistence probability go to zero in a stretched exponential manner. However, for $\kappa > 1$, although the system reaches the ground state after long time, the dynamical exponent and the persistence exponent are both different from that of the Ising model with nearest-neighbor interactions only [13].

In two or higher dimensions, zero-temperature quenching dynamics of Ising model with the nearest-neighbor interaction is also interesting. The system does not always reach the ground state and frozen-in striped states appear [11]. In three dimensions, the system never reaches the ground state [19]. Different interesting dynamical behaviors inspired the study of zero-temperature Glauber dynamics for the two-dimensional ANNNI model in which a competing interaction is present along one (horizontal) direction. The Hamiltonian of the model on the $L \times L$ lattice is given by

$$H = -J_0 \sum_{i,j=1}^{L} S_{i,j} S_{i+1,j} - J_1 \sum_{i,j=1} [S_{i,j} S_{i,j+1} - \kappa S_{i,j} S_{i,j+2}]. \quad (1)$$

For $\kappa < 1$, this system does not reach the equilibrium ground state (the ground state is ferromagnetic for $\kappa < 0.5$, and for $\kappa > 0.5$ antiphase order exists only in the horizontal direction; on the other hand, the vertical direction is always ferromagnetic), but slowly evolves to a metastable state. For $\kappa \geqslant 1$, both the persistence probability and the number of domain walls show algebraic decay. For $\kappa > 1$, the system shows a behavior similar to the two-dimensional ferromagnetic Ising model in the sense that it freezes to a striped state with a finite probability. However, for $\kappa = 1$, the system belongs to a completely different dynamical class and it always evolves to the true ground state with the persistence and dynamical exponent having unique values [15].

These above observations indicate that the two-dimensional Ising model with the competing interactions in both the vertical and horizontal directions may show rich dynamical behavior. In this work we have studied the dynamics of two-dimensional BNNNI (biaxial next-nearest-neighbor Ising) model where in addition to the ferromagnetic nearest-neighbor interaction, we have antiferromagnetic next-nearest-neighbor interaction in both x and y directions. The description of the model and the equilibrium properties has been discussed in detail in the next section. We indeed found three dynamical regions depending on the values of κ, the ratio between the antiferromagnetic and ferromagnetic interactions. For $\kappa < 1$, the system never reaches the ground state and remains active forever. For $\kappa \geqslant 1$, the system reaches the ground state with some probability less than *one*, and the probability of reaching the ground state is different for $\kappa > 1$ and $\kappa = 1$.

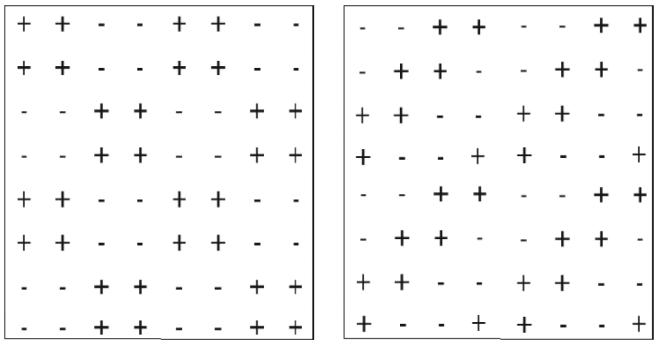

FIG. 1. The antiphase ground state (temperature $T = 0$) structures for $\kappa > 0.5$. First picture shows the "chessboard" type and the second one is "staircase" type. + and − signs stand for the up and down spin, respectively.

The paper is organized as follows: In Sec. II, we have described the model and its known properties. In Sec. III, we have given a list of the quantities we have computed for studying the dynamical evaluation. In Sec. IV, we have discussed the dynamic behavior in detail. The discussions and conclusions are made in the last section.

II. MODEL

The most generalized Hamiltonian for the two-dimensional BNNNI model could be given by

$$H = -J_0 \sum_{i,j=1}^{L} [(S_{i,j} S_{i+1,j} + S_{i,j} S_{i,j+1}) - \kappa (S_{i,j} S_{i+2,j} + S_{i,j} S_{i,j+2})], \quad (2)$$

where κ is the ratio of the next-nearest-neighbor antiferromagnetic interaction and the nearest-neighbor ferromagnetic interaction, which is same for both the x and y directions. The thermal phase diagram for two-dimensional BNNNI model is not exactly known, but the ground state structures are known and quite interesting. The ground state is completely ferromagnetic for $\kappa < 0.5$ and there exists antiphase order in both the vertical and horizontal directions for $\kappa > 0.5$. However, the ground state for $\kappa > 0.5$ can have two possible structures which contain the antiphase order in both the directions. These structures which have been illustrated in Fig. 1 are known as "chessboard" [Fig. 1(a)] and "staircase" [Fig. 1(b)] configurations [20].

Again, the ground state is infinitely degenerate at the fully frustrated point $\kappa = 0.5$

III. QUANTITIES COMPUTED

To study and analyze the dynamical properties of the system following a zero-temperature quench, we have computed the following quantities in this work:

(1) Residual energy $\varepsilon(t)$. For studying the dynamics of this model, the measurements of the domain walls are not very significant. As the ground state has the antiphase order in both the directions (off course for $\kappa > 0.5$), the number of domain

walls of the final state is the same as that of the average number of domain walls of the initial state and the number of domain walls does not decay with time. Although the number of domain walls remains almost constant, the energy of the system changes with time (for any value of κ) and the system self-organizes to find out its minimum energy state. Hence, instead of the number of domain walls, the appropriate measure for studying this ordering dynamics is the residual energy per spin $\varepsilon = E - E_0$, where $E_0 = -4J_0(1-\kappa)$ (for $\kappa < 0.5$) and $E_0 = -4J_0\kappa$ (for $\kappa > 0.5$) are the known ground state energy per spin and E is the energy of the dynamically evolving state.

The presence of domain walls in regular lattices causes an energy cost [16]. It has been shown before for the two-dimensional Ising model that the residual energy has the same scaling as that of the number or fraction of domain walls D_w [17,21]:

$$\varepsilon \sim t^{-1/z}.$$

Hence, computing the residual energy one can determine the value of the dynamical exponent z. Here, we will call z as ordering exponent instead of the domain growth exponent.

(2) Persistence probability $P(t)$. As mentioned earlier in the Introduction, it is the probability that a spin does not flip until time t. If persistence probability decays in a power law with time, that is $P(t) \sim t^{-\theta}$, the scaling form which can be used for finite size scaling is as follows [22,23]:

$$P(t, L) \sim t^{-\theta} f(L/t^{1/z}). \tag{3}$$

For $x \ll 1$ the scaling function $f(x) \sim x^{-\alpha}$ with $\alpha = z\theta$. For large x, $f(x)$ is a constant. Hence, it is clear that for finite systems, the persistence probability saturates and the saturation value $P_{\rm sat} \sim L^{-\alpha}$ at large times ($t \to \infty$). The value of the exponent z obtained from the scaling of the residual energy should satisfy the scaling relation given by Eq. (3).

It has been previously shown that the exponent α is related to the fractal dimension of the fractal formed by the persistent spins [22]. The fractal dimension $d_f = d - \alpha$, where d is the dimension of the system. Here, we have obtained an estimate of α and hence d_f using the above scaling form of Eq. (3).

(3) Autocorrelation $A(t)$. The autocorrelation function measures the correlation of the state of a single spin at time t with its state at a previous time. The functional form of it is defined as

$$A(t) = \frac{\langle S_i(t)S_i(t_0)\rangle_i - \langle S_i(t)\rangle_i \langle S_i(t_0)\rangle_i}{\sigma_i(t)\sigma_i(t_0)}, \tag{4}$$

where $S_i(t)$ and $S_i(t_0)$ are the states of the spin i at time t and t_0, respectively. $\langle \dots \rangle_i$ is the average over i index; and $\sigma_i(\dots)$ is the standard deviation over i index. We have studied the decay of autocorrelation for the system with the initial time only. That is, $t_0 = 0$ for Eq. (4).

For the nearest-neighbor Ising model the autocorrelation function scales as [24]

$$A(t) \sim t^{-\lambda/z}, \tag{5}$$

where λ is the autocorrelation exponent and z is the ordering exponent same as that of given by the scaling of residual energy and Eq. (3). We have studied the decay of the autocorrelation function not only for the BNNNI model, but also for ANNNI spin system [Eq. (1)] for different values of κ.

(4) Probability that the system will *not* reach the ground state $P_{\rm str}$ and the probability that the system will remain in the active state after very long time $P_{\rm act}$. These quantities have been computed by computing the percentage of the configurations which have not reached the ground state starting from an initial random state $P_{\rm str}$ and the percentage of the configurations which remained active after a very long time $P_{\rm act}$.

We have taken lattices of size $L \times L$ with $L = 40,\ 80,\ 132,$ and 200 to study the dynamical behavior of the system. The behavior of different quantities which decays with time (residual energy, persistence, and autocorrelation) has been averaged over at least 500 configurations for each lattice size. For estimating $P_{\rm str}$ and $P_{\rm act}$, we have averaged over a much larger number of initial configurations (of the order of 4000). Periodic boundary condition has been used in both x and y directions. $J_0 = 1$ has been used in the numerical simulations.

IV. DYNAMICAL BEHAVIOR IN DETAIL

Before discussing the dynamical behavior in detail, let us first discuss the stability of simple spin configurations which will help us to realize that the dynamical behavior of the system is strongly dependent on κ.

A. Stability of simple spin structures

It is more or less well understood that the zero-temperature dynamics of Ising spin system is mostly determined by the stability of spin configurations locally. Hence, the system can freeze with such spin configurations which do not correspond to global minimum of energy, but still can be stable dynamically. The well known example of this is the presence of striped state for two- or higher-dimensional Ising model with nearest-neighbor interaction and ANNNI model [for $\kappa > 1$, Eq. (1)]. Although these configurations are stable, they do not correspond to the global minimum of energy.

For the dynamics of the BNNNI model, the fate of a randomly selected spin is determined by the state of its eight neighbors which could be in any one of the $2^8 = 256$ possible configurations. Although, for many of these configurations the dynamical behavior of the central spin is similar for any given value of κ. For example, if among the four nearest neighbors, two of them are up and the other two are down or vice versa, the state of central spin will be determined by the configurations (which could be any one of the $2^4 \times 6 = 96$ configurations) of the next-nearest neighbors. For the similar configurations of the next-nearest neighbors, the dynamics will be determined by the orientations of the nearest neighbors only. Except for these cases, for most of the configurations the fate of a randomly selected spin will depend on the values of κ and we will see that one can expect the similar dynamical behavior for a range of κ values. We should also remember that for having a stable configuration locally, not only the randomly selected spin, but also its eight neighbors have to be stable.

First, let us consider the simplest configuration of a single up spin in a sea of down spins [Fig. 2(a)] or vice versa.

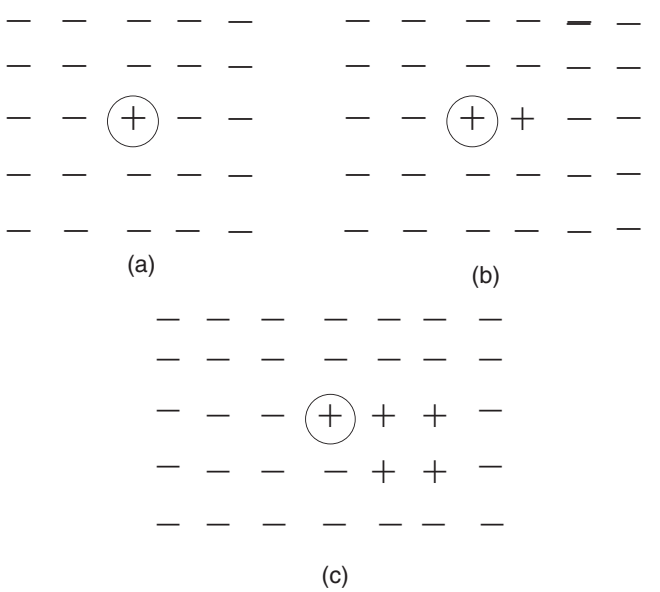

FIG. 2. Schematic diagram of the spin configurations for the analysis of stability of simple structures: the conditions for the stability of the central spin (which have been circled) and its neighbors have been discussed in the text.

The central spin will be stable for $\kappa > 1$ and is unstable for $\kappa < 1$. For $\kappa = 1$, the spin will flip with probability $1/2$, hence making the dynamics stochastic. However, all its four nearest neighbors are stable only for $\kappa < 0.5$. On the other hand, four next-nearest neighbors of the central spin are stable when $\kappa < 2$. Now, for a domain of two up spins in a sea of down spins [as shown in Fig. 2(b)], both the up spins will be stable for $\kappa > 0.5$. But, the down spins at their nearest neighbors (like the three nearest neighbors of the circled spin which are at the down state) will be stable when $\kappa < 0.5$. On the other hand, for the four next-nearest neighbors, three of them will be stable as long as $\kappa < 2$ and one of them will be stable for $\kappa < 1$.

Next, we would like to consider the configuration of a domain of five up spins in a sea of down spins [Fig. 2(c)]. The spin at the corner of the domain of up spins (it has been circled) will be stable for $\kappa > 1$ only. The up spin at the right nearest neighbor of this circled spin will be always stable for any value of $\kappa > 0$. But, the down spin at the left nearest neighbor will be stable only for $\kappa < 1$. The other two down spins at the nearest neighbor of the circled spin will be stable as long as $\kappa < 0.5$. Among the next-nearest neighbors of the circled spin, the up spin will be stable for any value of $\kappa > 0$, but all the down spins will be stable whenever $\kappa < 2$.

One can consider more complicated structures, but the analysis of these simple structures indicates that there could be different dynamical behavior in the region $\kappa < 1$, $\kappa = 1$, $\kappa > 1$, $\kappa = 2$, and $\kappa > 2$. However, as far as the dynamical behavior of the system (that means the behavior of all the quantities we have computed including residual energy, persistence, autocorrelation function, etc.) is concerned, we find that there exist only three regions with different dynamical behavior: $\kappa < 1$, $\kappa = 1$, and $\kappa > 1$.

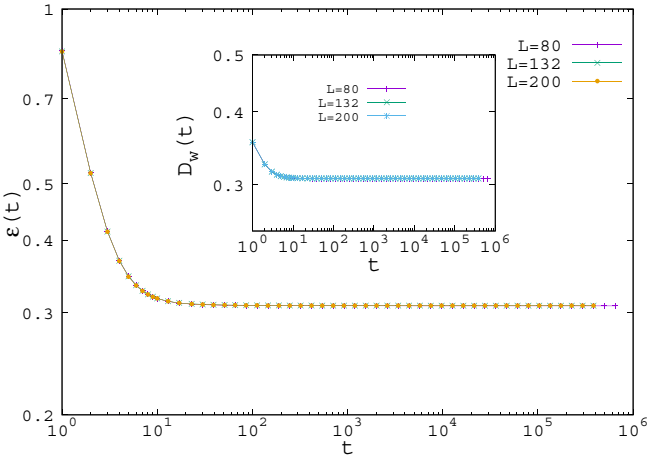

FIG. 3. Decay of the residual energy $\varepsilon(t)$ with time for $\kappa = 0.6$. Fraction of domain walls as a function of time for the same value of κ has been plotted in the inset.

We have also studied the decay of the autocorrelation function for the ANNNI model [Hamiltonian is given by Eq. (1)], which has been discussed and compared with BNNNI in the last subsection of this section.

B. Dynamics in the region $0 < \kappa < 1$

Although from the analysis of the simple spin structures one can guess that the dynamical behavior could be different for $\kappa < 0.5$ and $\kappa > 0.5$, we find that the system has identical dynamical behavior for all κ, in the region $0 < \kappa < 1$. At this parameter regime, the system does not go to its equilibrium ground state at all making $P_{\rm str}$ to be *one* for all the values of κ. At the beginning of the dynamics, domains of size one will vanish rapidly. After that, for the above mentioned reasons, the dynamics will be bit complex and slow, but will continue for a long time.

The fraction of domain walls $D_w(t)$ decays very little in both the directions at the initial time and then remains constant for the rest of the dynamics (inset of Fig. 3). The residual energy also stops decaying after some time but the dynamics

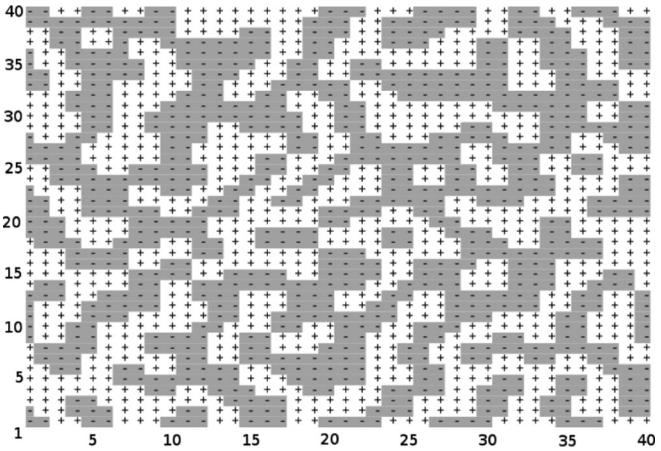

FIG. 4. Snapshot of 40×40 lattice at time $t = 10$ for $0 < \kappa < 1$. $+$ and $-$ signs stand for the up and down spin, respectively.

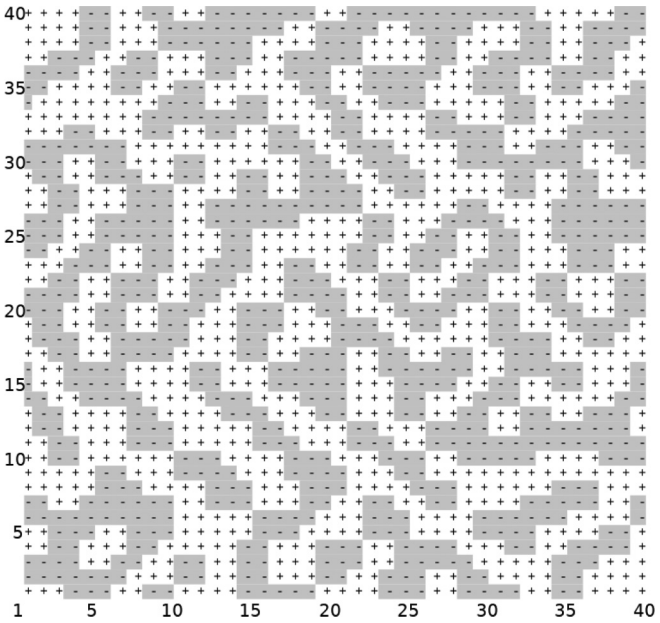

FIG. 5. Snapshot of 40×40 lattice at time $t = 50$ for $0 < \kappa < 1$. $+$ and $-$ signs stand for the up and down spin, respectively.

continues. It is prominent from Fig. 3 that finite size effects do not exist for the decay of residual energy and the fraction of domain walls.

Figures 4–7 are the snapshots of the system at different times which shows the evolution of the typical lattice structures at this parameter regime after a quench to zero temperature.

From a very early time, diagonal stripelike structures will appear in the lattice which will remain forever. These diagonal stripes become more prominent in the lattice with time as the dynamics continues even after the residual energy stops decaying.

After some initial time (for $t > 300$, Fig. 3), spin flips do not reduce the energy of the system and, hence, the residual energy stops decaying. Although the energy of the system does not decay anymore, a few of these spins remain active for a very long time, even at $t \to \infty$ making $P_{\rm act} = 1$ for any values of $\kappa < 1$. Some of those spins have been highlighted in the red color box in Figs. 6 and 7.

The active sites (the sites at which the spins keep flipping) move throughout the lattice along the edge of the poorly formed diagonal stripes, killing the persistence of all the sites of the lattice. Persistence probability for $\kappa < 1$ shows a slow decay with time and goes to *zero* at long time. The functional form for the decay is different at the beginning and at the end of the dynamics. At the beginning of the dynamics, the decay is slower than that of the later time and the functional form can be approximated as $g(x) \sim t^{-c} \times \ln(bt)$ for an appreciable range of time. We have numerically found that the function $g(x)$ fits well at the beginning of the dynamics with $b \simeq 2.266$ and $c \simeq 0.515$ (Fig. 8). However, at late time, it is not possible to characterize the decay of the persistence probability by some simple mathematical function of time. The decay of the persistence probability does not have any effect on the finite system sizes (Figure. 8).

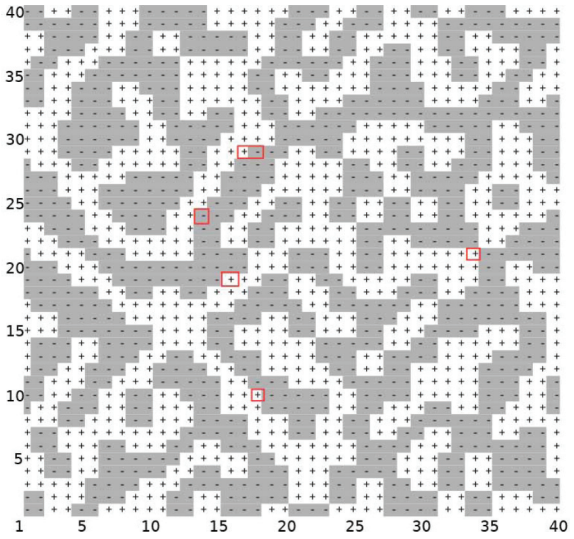

FIG. 6. Snapshot of 40×40 lattice at time $t = 500$ for $0 < \kappa < 1$. $+$ and $-$ signs stand for the up and down spin, respectively.

We have also studied the decay of the autocorrelation function with time for this parameter region. The results for that have been presented in the last subsection of this section.

C. Dynamics for $\kappa > 1$

It had been previously observed for axially next-nearest-neighbor Ising model with the competing interactions (that is ANNNI model) that the dynamical behavior changes drastically at $\kappa = 1$ in both one and two dimensions. For the two-dimensional BNNNI model, the presence of competing interaction in both the directions has an effect on the dynamics in a large extent. As mentioned before, like the ANNNI

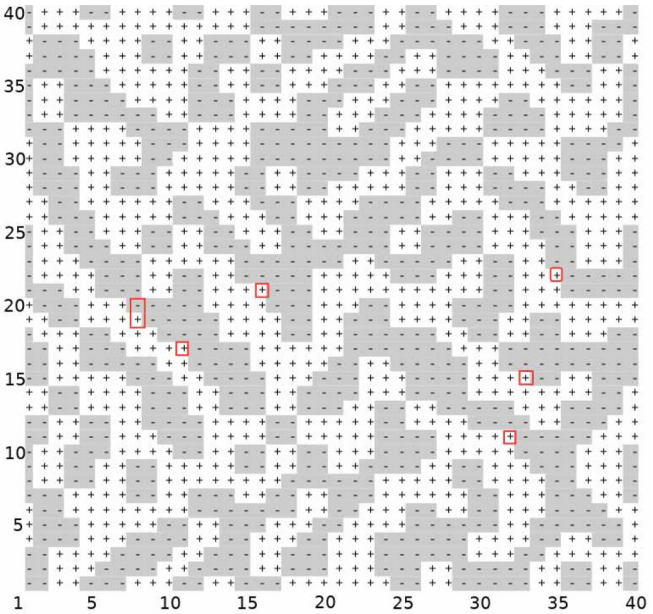

FIG. 7. Snapshot of 40×40 lattice after a very long time that is at $t \to \infty$ (at $t = 500\,000$) for $0 < \kappa < 1$. $+$ and $-$ signs stand for the up and down spin, respectively.

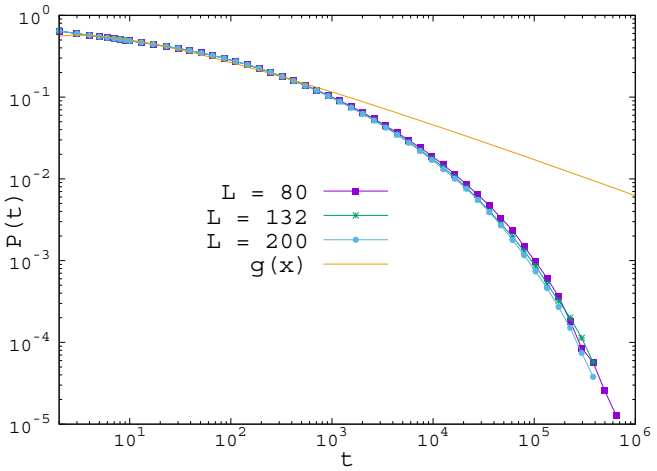

FIG. 8. Decay of the persistence probability with time for $\kappa < 1$. The fitting of the approximated functional form [the form of the function $g(x)$ is given in the text] has been shown at the beginning of the dynamics for an appreciable range of time.

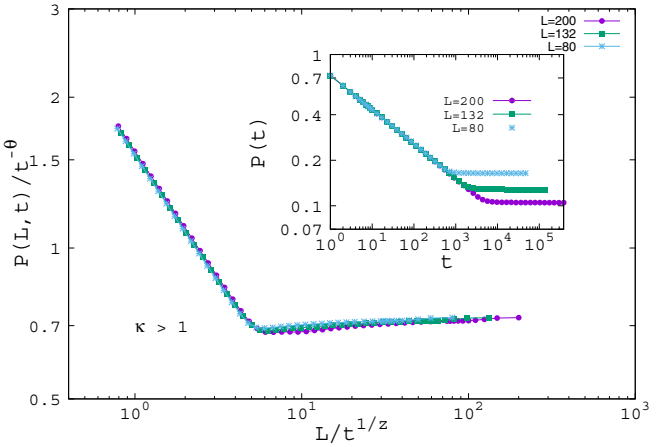

FIG. 10. The collapse of scaled persistence data versus scaled time using $\theta = 0.22$ and $z = 2.33$ is shown for different system sizes for $\kappa > 1$. Inset shows the unscaled data for the decay of the persistence probability with time.

model, the dynamical behavior of the BNNNI model is also different for $\kappa = 1$ and $\kappa > 1$. In this section we will discuss the dynamical behavior of the model for $\kappa > 1$.

The number of domain walls does not much change with time and quickly saturates at a value 0.5 for the fraction of the domain walls, in both the horizontal and vertical directions. Although the domain walls saturate very early, residual energy decays in a power law in time, with a decay exponent $\sim$0.43 (Fig. 9). This yields the ordering exponent $z \simeq 2.33$ as $\varepsilon \sim t^{-1/z}$. In the inset of Fig. 9, we have also shown the decay of the residual energy for the two-dimensional nearest-neighbor Ising model.

It is clear from the saturation of the residual energy that some kind of striped states exist in the system in this parameter regime. Just before the saturation, residual energy shows an exponential decay for some small time. This is due to the

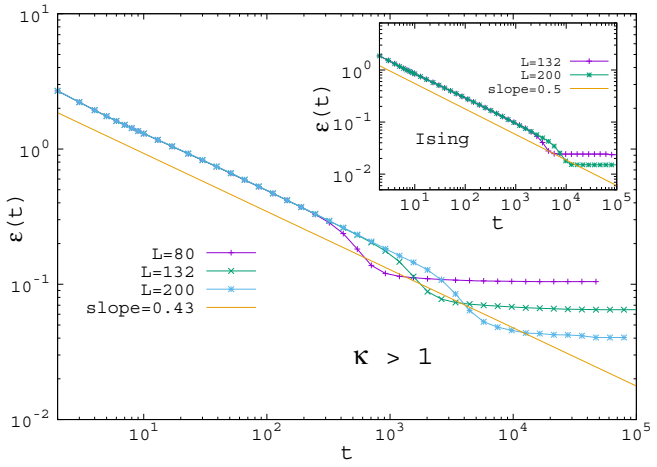

FIG. 9. Decay of the residual energy with time for $\kappa > 1$. The amber color line has a slope 0.43 in the main plot. Inset shows the decay of the residual energy with time for two-dimensional nearest-neighbor Ising model. The amber color line has a slope 0.5 at the inset.

exponential decay of ε for those configurations which go to the ground state instead of getting freezed in one of the striped states. Saturation of residual energy (and an exponential decay of it just before the saturation) for two-dimensional nearest-neighbor Ising model (inset of Fig. 9) is also due to the presence of the striped state in the lattice [11].

Persistence probability decays in a power law in time and the persistence exponent $\theta \simeq 0.22$. One can expect $z \simeq 2.33$ from the finite size scaling analysis, if the ordering exponent z is similar to that of the previously known domain growth exponent. We indeed found $\theta = 0.22 \pm 0.002$ and $z = 2.33 \pm 0.01$ performing the finite size scaling analysis following Eq. (3) and we have checked this for different values of κ ($\kappa = 1.3,\ 1.6,\ 2.0,\ 2.5$, and 20). So, we conclude that these exponents are independent of κ for $\kappa > 1$ and also the ordering exponent z is similar to the dynamical exponent which is previously known as the domain growth exponent. A typical behavior of the raw persistence data as well as the data collapse for the finite size scaling is shown in Fig. 10.

Next, we asked what is the probability $P_{\rm str}$ that the system will *not* reach the ground state and will freeze in one of the striped states. This has been calculated by computing the fraction of the initial configurations which could not reach the ground state (those states have *nonzero* residual energy) at all after a very long time.

We found that little more than 80% of the configurations freeze to some striped states before reaching the ground state. The freezing probability $P_{\rm str}$ initially increases with system sizes and then saturates for larger systems (Fig. 11). We did not find any significant differences in the values of $P_{\rm str}$ for larger sizes for $\kappa > 1$. It may appear from Fig. 11 that the freezing probability has different saturation values (the values for large enough system sizes) for $1 < \kappa < 2$ and $\kappa \geqslant 2$, but the difference between these two values is insignificant ($P_{\rm str} \simeq 81.5\%$ when $1 < \kappa < 2$ and $P_{\rm str} \simeq 81\%$ for $\kappa \geqslant 2$). We also found that for the configurations which reach the ground state, half of them reach the checkerboard configuration and the other half reach the staircase configuration.

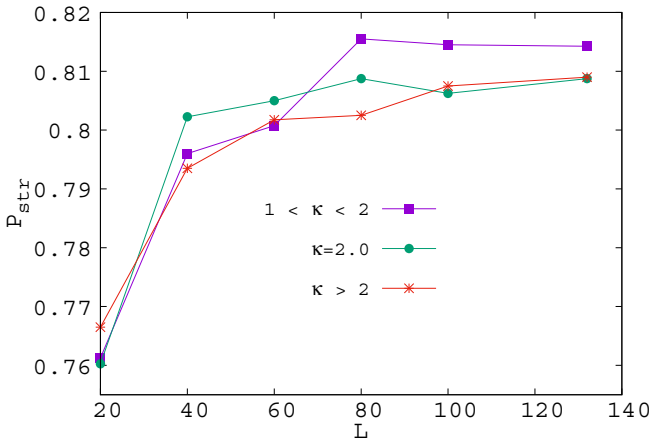

FIG. 11. Freezing probability P_{str} is plotted with the system size for a different range of κ values.

P_{act}, the probability of being in the active state after a very long time, is equal to *zero* for any values of κ for $\kappa > 1$. That means all the configurations either go to the striped state (with no active state or site in it) or to one of the ground states at $t \to \infty$.

It is not straightforward to imagine the structure of the striped states appearing in the lattice after it reaches the steady state at the end of the dynamics. We found that the checkerboard configuration and the staircase configuration stay together in the lattice. The energy cost at the interface of these two configurations is more than the energy of the ground state, although these interfaces are stable for $\kappa > 1$. A typical snapshot of this type of striped state which appears for $\kappa > 1$ has been shown in Fig. 12.

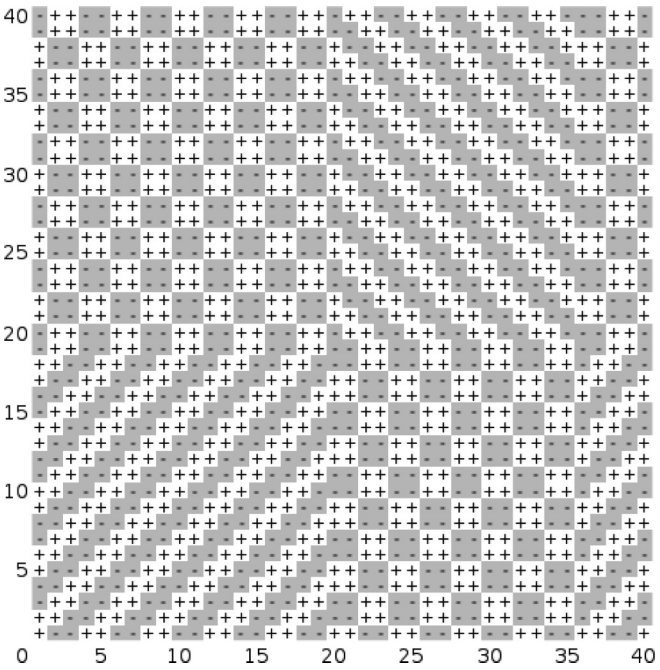

FIG. 12. A typical snapshot of the striped state for $\kappa > 1$ after the system reaches the steady state configuration.

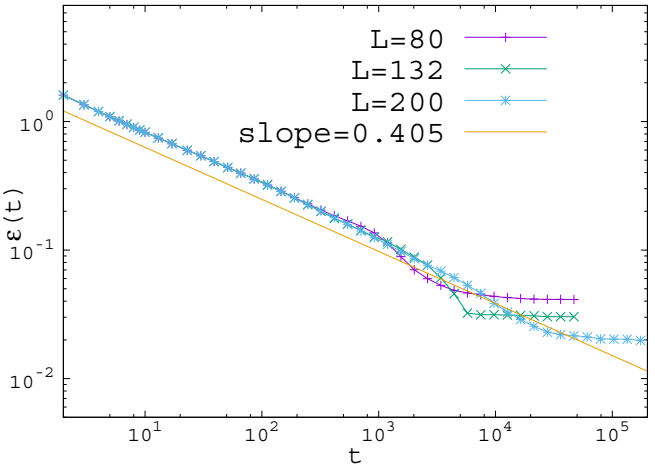

FIG. 13. Decay of the residual energy with time for $\kappa = 1$. The amber color line has a slope 0.405.

Also, for this parameter region, we have studied the decay of the autocorrelation function with time. However, the results for that have been presented in the last subsection of this section.

D. Dynamics for $\kappa = 1$

Residual energy decays in a power law with time and from the decay we found that the ordering exponent z to be close to 2.47 (Fig. 13) which is significantly different from the value of z for $\kappa > 1$. Saturation value of the residual energy indicates that also for $\kappa = 1$, the striped state exists in the system after it reaches the steady state. This phenomenon is contrary to what happens in the two-dimensional ANNNI model [15] for $\kappa = 1$ where the system reaches the ground state with probability *one*.

Persistence probability decays in a power law with the exponent $\theta = 0.332 \pm 0.002$. The finite size scaling suggests the ordering exponent $z = 2.47 \pm 0.04$ and the value is consistent with what we get from the decay of residual energy. A typical behavior of the raw persistence data as well as the data collapse using the finite size scaling analysis is shown in Fig. 14. The quality of the data collapse is *not* as good as that of $\kappa > 1$, which gives a higher error bar on the ordering exponent z.

We found that less than 1% of the configurations remain active after a very long time for the higher sizes making P_{act} to be very low. The probability for a configuration to be in an active state is almost zero for the lower system sizes. Just like $\kappa > 1$, here also we asked about the probability (P_{str}) that a system will not reach the ground state. In this case, either it will freeze in one of the striped states or it will end up in one of the rare active states. We found that little more than 50% configurations fail to reach the ground state even after a very long time (Fig. 15). The configurations which reach the ground state, surprisingly almost 80% (being precise 79% according to the numerical estimate we obtained) of them reach the checkerboard configuration and little more 20% configurations reach the staircase configuration (inset of Fig. 11).

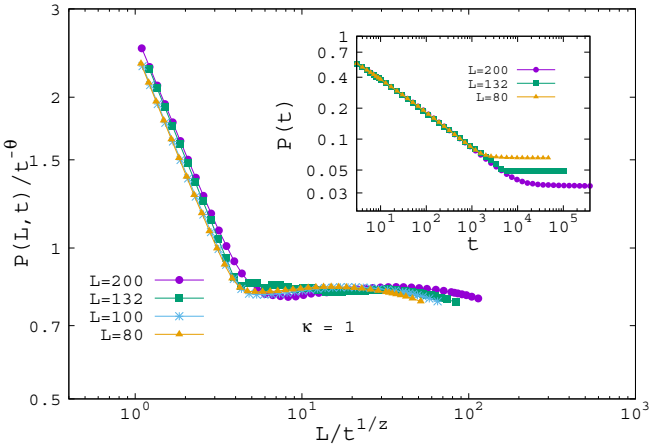

FIG. 14. The collapse of scaled persistence data versus scaled time using $\theta = 0.332$ and $z = 2.48$ is shown for different system sizes for $\kappa = 1$. Inset shows the unscaled data for the decay of the persistence probability with time.

As we have mentioned earlier, in case of large system sizes very few configurations can remain active even after a very long time. These long lived configurations are actually diagonal stripe configurations which had been previously observed to appear in the two-dimensional Ising model [11]. But, the dynamics for these configurations is much more complicated than that of the two-dimensional Ising model. These configurations will eventually go to the ground state. But, it is not simple to argue as to how much time is required for this configuration to reach the ground state.

Although it is not trivial to detect these rare configurations, we have shown a typical snapshot of this kind of active configuration in Fig. 16. Usually, all the neighbors of the active lattice sites (circled in red color in Fig. 16) are stable except one. If the active site flip (it will flip will probability 1/2 as the energy for that site is *zero*), the unstable neighbor becomes stable and one stable neighbor becomes unstable

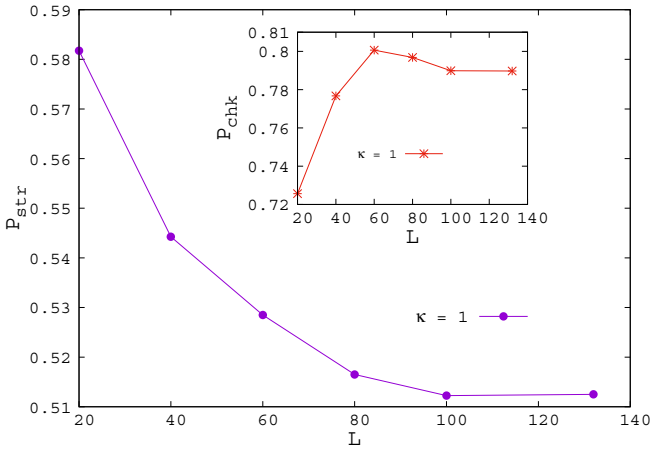

FIG. 15. Freezing probability $P_{\rm str}$ is plotted with the system size for $\kappa = 1$. Variation of $P_{\rm chk}$, the probability for a system to reach the checkerboard configuration if it reaches the ground state, has been plotted against the system size L at the inset.

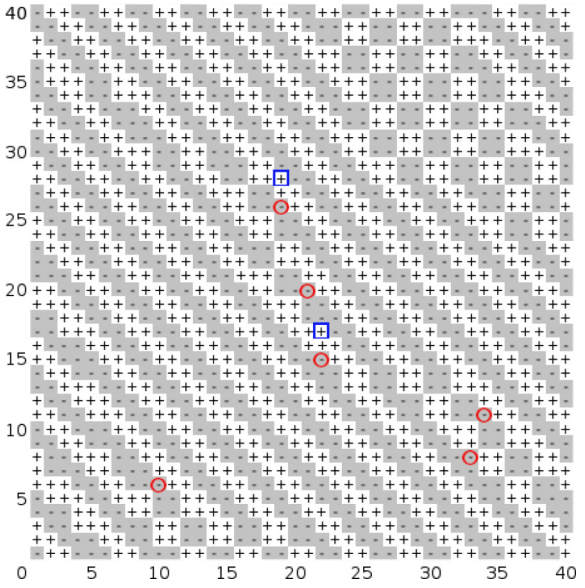

FIG. 16. A typical snapshot of an active configuration after a very long time for $\kappa = 1$. Few of the active sites have been circled in red color.

(shown in blue square in Fig. 16). This is how the active sites move in the lattice in a pair unless a local configuration for the definite flip has formed in the lattice. The mechanism makes the dynamics very slow at this point of time. Time taken by the system to reach the ground from this kind of active configuration is an order of magnitude higher than other configurations and computing the time is beyond the available computational power.

E. Decay of autocorrelation function

In this section we present the results for the decay of autocorrelation function with time for different values of κ. To compare the results we have studied the time decay of the function also for the ANNNI model [given by Eq. (1)], as that has not been studied before in [15]. For two-dimensional

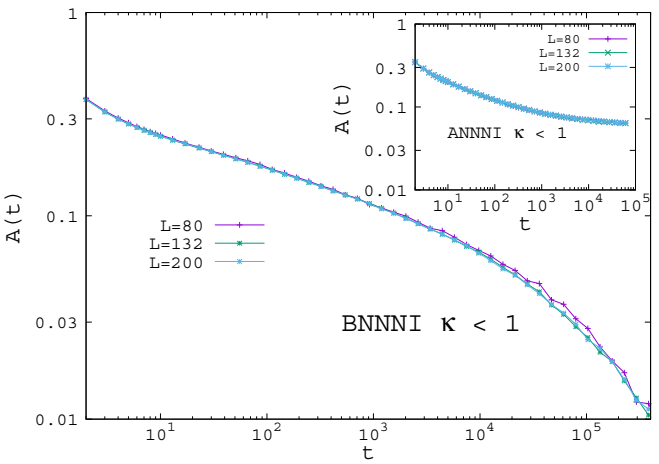

FIG. 17. Decay of autocorrelation function with time for $\kappa < 1$. Inset shows the same for the ANNNI model.

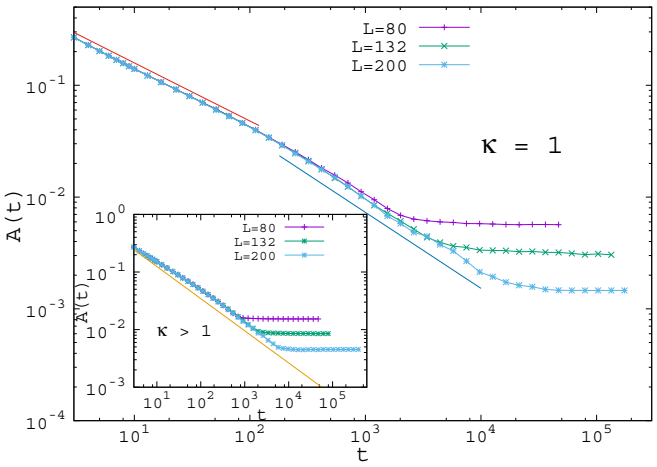

FIG. 18. Decay of the autocorrelation function with time has been plotted for $\kappa = 1$ in the main plot. The slope of the red line at the beginning is 0.52 and the slope of the blue line in the same plot is 0.68. Inset shows the decay for $\kappa > 1$, where the slope of the yellow line is 0.558.

nearest-neighbor Ising model (which corresponds to $\kappa = 0$), the value of the autocorrelation exponent $\lambda \simeq 1.25$ [25] has been verified from our numerics.

For $\kappa < 1$, the autocorrelation function does not decay in a power law fashion for both the BNNNI and ANNNI models (Fig. 17). For the BNNNI model, the autocorrelation function slowly decays to zero, though it is almost impossible to write any simple mathematical form for the decay of the function with time. For the ANNNI model the autocorrelation function also shows a slow decay with time, however, that can be approximated by $1/\log(t)$ for an appreciable range of time. At larger time, it saturates at a finite value unlike the BNNNI model.

For $\kappa \geqslant 1$, the autocorrelation function shows a power law decay with time, with different decay exponent for $\kappa = 1$ and

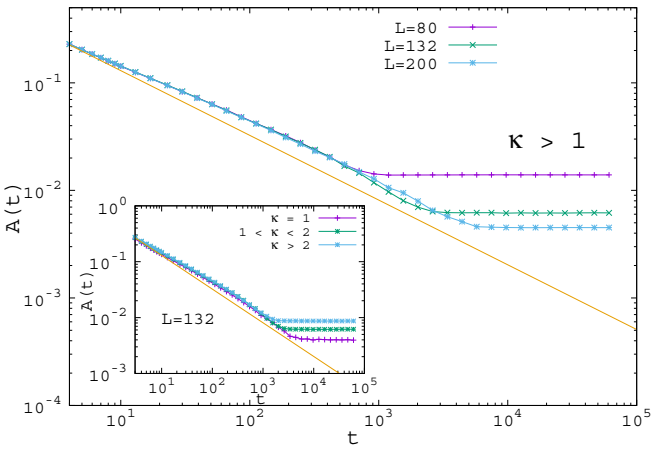

FIG. 19. Decay of the autocorrelation function with time for different sizes has been plotted for $\kappa > 1$ in the case of the ANNNI model. Inset shows that the decay exponent is the same for any value of $\kappa \geqslant 1$ for ANNNI. The slope of the amber colored line is 0.602 for both the main plot and inset.

$\kappa > 1$. For $\kappa > 1$, it decays as $t^{-\eta}$ with $\eta = 0.558 \pm 0.002$ after some initial time (inset of Fig. 18). This yields the autocorrelation exponent $\lambda = 1.3 \pm 0.01$ as $\eta = \lambda/z$ [Eq. (5)] as $z = 2.33 \pm 0.01$ (Sec. IV C). However, for $\kappa = 1$, the decay exponent appears to be different for some initial time and at the large time. At the beginning, it decays as $t^{-\eta}$ with $\eta = 0.521 \pm 0.002$ giving $\lambda = 1.29 \pm 0.025$ as $z = 2.47 \pm 0.04$ (Sec. IV D). At long time the decay exponent $\eta = 0.68 \pm 0.002$, which corresponds to the autocorrelation exponent $\lambda = 1.68 \pm 0.03$.

On the other hand, in case of the ANNNI model for $\kappa \geqslant 1$ the autocorrelation function has a power law decay with same decay exponent η for both $\kappa = 1$ and $\kappa > 1$. However, as the value of z is different for $\kappa = 1$ and $\kappa > 1$ [15], the autocorrelation exponent will be different. We found $A(t) \sim t^{-\eta}$ with $\eta = 0.602 \pm 0.002$ for $\kappa \geqslant 1$ (Fig. 19). That concludes $\lambda = 1.11 \pm 0.01$ for $\kappa = 1$ (as $z = 1.84 \pm 0.01$ [15]) and $\lambda = 1.25 \pm 0.01$ for $\kappa > 1$ (as $z = 2.08 \pm 0.01$ [15]) for the ANNNI model.

V. DISCUSSIONS AND CONCLUSIONS

We have studied the dynamical features of the BNNNI model in two dimensions following a quench to zero temperature. We have seen that the dynamics is very much dependent on the value of κ, the ratio of the antiferromagnetic to the ferromagnetic interaction in both the directions. Depending on the dynamical features we can distinguish three different regimes $\kappa < 1$, $\kappa = 1$, and $\kappa > 1$ just like the ANNNI model in two dimensions. Although the intrinsic dynamical behavior of the model is a bit different from that of ANNNI. Presence of the competing interaction in both the vertical and horizontal directions (which make the model symmetric unlike ANNNI) can affect the dynamics substantially. For example, unlike the ANNNI model, here the system remains in the active state forever when $\kappa < 1$.

For studying the dynamics of ordering after a quench to zero temperature, we have studied the decay of the residual energy, as domain walls do not decay with time. When residual energy has power law decay (that is for $\kappa \geqslant 1$), we claim that the decay exponent is similar to that of the domain growth exponent z. We have obtained the data collapse of persistence data for $\kappa \geqslant 1$ successfully, using the value of the dynamical exponent z acquired from the power law decay of residual energy. As the system organizes itself to find out its minimum energy state despite of the fact that the traditional domain growth phenomena does not happen, we have called the exponent z as ordering exponent.

For $\kappa > 1$, we found the persistence exponent θ to be the same as that of the two-dimensional nearest-neighbor Ising model (corresponding to $\kappa = 0$), though the value of the ordering exponent z is a bit different. This makes the exponent $\alpha = z\theta$ to be very different for $\kappa = 0$ and $\kappa > 1$. For $\kappa = 0$, $\alpha \simeq 0.44$ while for $\kappa > 1$, $\alpha = 0.512 \pm 0.005$. This tells us that the spatial correlations of the persistent spins are quite different for the two and not only the dynamical class for $\kappa = 0$ and $\kappa > 1$ are different (which is already evident from the difference in the value of z), also the persistence behavior is not the same. $\kappa = 1$ appears to be a special point where the dynamic behavior changes radically with a different value of

θ and z than that of $\kappa = 0$ and $\kappa > 1$. Here, we obtained the value of α to be 0.82 ± 0.018. The error bar is higher as an effect of having a higher error bar on z for $\kappa = 1$.

Next, we would like to comment on the behavior of the autocorrelation function. We have studied the decay of the function with time from which we have obtained the values of the autocorrelation exponent λ (for $\kappa \geqslant 1$, when the function has a power law decay), using the value of z. We have studied this not only for BNNNI, but also for the ANNNI model, which is anisotropic by nature. For BNNNI model, when $\kappa > 1$, the value of λ is close but different from that of $\kappa = 0$. However, for ANNNI, the value of λ obtained from our numerics is similar to the two-dimensional nearest-neighbor Ising model. For $\kappa = 1$, the autocorrelation exponent λ appears to be different at the beginning and at the end of the dynamics. At the beginning, λ is almost the same as that of $\kappa > 1$, though at late time the value of λ is very different and higher than that. On the other hand, in case of the ANNNI model for $\kappa = 1$, the value of λ is lower than that of $\kappa > 1$ and $\kappa = 0$.

It is important to note that the system always reaches an absorbing state for $\kappa > 1$ and remains in the active state when $\kappa < 1$. For $\kappa = 1$, most of the configurations go to the absorbing state except a very few long lived configurations. These rare configurations reach the absorbing state taking a very long time, which is an order of magnitude higher than the time taken by other configurations. This indicates that there may exist an active to absorbing phase transition around $\kappa = 1$. This type of behavior for zero-temperature single spin flip dynamics has been observed before for the one-dimensional ANNNI model (which is also isotropic by nature), where the system remains in the active state for $\kappa < 1$ and reaches the absorbing state for $\kappa \geqslant 1$. Hence, if an active to absorbing phase transition exists, that can be checked and studied in detail as a separate problem in future. Also, for $\kappa = 1$, estimating the time taken by the long lived configurations to reach the absorbing state can be the part of the problem of future study.

The single spin flip dynamics for the BNNNI and ANNNI models can also be studied in three and higher dimensions. The dynamical structure of the three-dimensional nearest-neighbor Ising model after a quenching to zero temperature is already complex and a bit interesting [19]. Hence, one can expect novel dynamical behavior for three-dimensional BNNNI and ANNNI models too. Also following the hypothesis which has been noted in the previous paragraph, there should not exist any plausible active to absorbing phase transition in three dimensions for these models as both models do not remain isotropic in the higher dimension.

In this paper, we have studied the dynamical behavior of the two-dimensional BNNNI model under a zero-temperature quench. The dynamics at finite temperature can be quite different. As the spin flipping probabilities are stochastic at finite temperatures, and the dynamical frustration for which the system freezes before reaching its ground state can be overcome by the thermal fluctuations. We would also like to note that, given the definition of persistence being a bit different at finite temperatures [26], it is not simple to guess the persistence behavior (for any spatial dimension) just from the results of the zero-temperature quenching dynamics. The single spin flip dynamics of the BNNNI model after a quench to the finite temperature indeed remains as an open problem which could be addressed in the future.

ACKNOWLEDGMENTS

The authors thank D. Boyer for useful discussions and T. Gorin for a critical reading of a previous version of the paper. Both the authors would like to acknowledge the financial support from SEP under Prodep Program No. 238628, folio UDG-PTC-1307. The computational power provided by CIC-UNAM for some of the simulations has also been acknowledged.

[1] P. C. Hohenberg and B. I. Halperin, Rev. Mod. Phys. **49**, 435 (1977).
[2] *Nonequilibrium Statistical Mechanics in One Dimension*, edited by V. Privman (Cambridge University Press, Cambridge, 1997).
[3] S. Biswas, *Novel Dynamical Phenomena in Magnetic Systems* (Academic, New York, 2013).
[4] A. J. Bray, Adv. Phys. **43**, 357 (1994) and the references therein.
[5] R. J. Glauber, J. Math. Phys. **4**, 294 (1963).
[6] J. D. Gunton, M. San Miguel, and P. S. Sahni, *Phase Transitions and Critical Phenomena*, Vol. 8, edited by C. Domb and J. L. Lebowitz (Academic, New York, 1983).
[7] For a review, see S. N. Majumdar, Curr. Sci. **77**, 370 (1999).
[8] B. Derrida, A. J. Bray, and C. Godreche, J. Phys. A: Math. Gen. **27**, L357 (1994).
[9] D. Stauffer, J. Phys. A: Math. Gen. **27**, 5029 (1994).
[10] P. L. Krapivsky, E. Ben-Naim, and S. Redner, Phys. Rev. E **50**, 2474 (1994).
[11] V. Spirin, P. L. Krapivsky, and S. Redner, Phys. Rev. E **63**, 036118 (2001).
[12] S. Redner and P. L. Krapivsky, J. Phys. A: Math Gen. **31**, 9229 (1998).
[13] P. Sen and S. Dasgupta, J. Phys. A: Math. Gen. **37**, 11949 (2004).
[14] D. Das and M. S. Barma, Phys. Rev. E **60**, 2577 (1999).
[15] S. Biswas, A. K. Chandra, and P. Sen, Phys. Rev. E **78**, 041119 (2008).
[16] D. Boyer and O. Miramontes, Phys. Rev. E **67**, 035102(R) (2003).
[17] S. Biswas and P. Sen, Phys. Rev. E **84**, 066107 (2011).
[18] W. Selke, Phys. Rep. **170**, 213 (1988).
[19] J. Olejarz, P. L. Krapivsky, and S. Redner, Phys. Rev. E **83**, 030104(R) (2011).
[20] J. Oitmaa and M. J. Velgakis, J. Phys. A **20**, 1495, (1987); M. J. Velgakis and J. Oitmaa, *ibid.* **21**, 547 (1988).
[21] P. Svenson, Phys. Rev. E **64**, 036122 (2001); P. K. Das and P. Sen, Eur. Phys. J. B **47**, 391 (2005).
[22] G. Manoj and P. Ray, Phys. Rev. E **62**, 7755 (2000); J. Phys. A: Math. Gen. **33**, 5489 (2000).

[23] S. Biswas and P. Sen, Phys. Rev. E **80**, 027101 (2009).

[24] David A Huse, Phys. Rev. B **40**, 304 (1989); C. Sire and S. N. Majumdar, Phys. Rev. Lett **74**, 4321 (1995).

[25] J. Midya, S. Majumder, and S. K. Das, J. Phys.: Condens. Matter **26**, 452202 (2014); Fong Liu and Gene F. Mazenko, Phys. Rev. B **44**, 9185 (1991).

[26] B. Derrida, Phys. Rev. E **55**, 3705 (1997).